Journal of Alloys and Compounds 633 (2015) 333–337

Contents lists available at ScienceDirect

Journal of Alloys and Compounds

journal homepage: www.elsevier.com/locate/jalcom

Exchange-coupling in thermal annealed bimagnetic core/shell nanoparticles

G.C. Lavorato *, E. Lima Jr., H.E. Troiani, R.D. Zysler, E.L. Winkler

Centro Atómico Bariloche, CNEA-CONICET, 8400 S.C. de Bariloche, Río Negro, Argentina

ARTICLE INFO

Article history:
Received 12 January 2015
Received in revised form 5 February 2015
Accepted 6 February 2015
Available online 13 February 2015

Keywords:
Nanostructured materials
Chemical synthesis
Core–shell nanoparticles
Magnetization
Magnetic measurements
TEM

ABSTRACT

In this study we demonstrate that the effective coupling of the magnetic phases in core/shell nanoparticles can be promoted by an appropriate thermal annealing. In this way, the magnetization thermal stability of the hard ferrimagnetic $CoFe_2O_4$ oxide can be increased up to room temperature when coupled to a CoO antiferromagnetic core in an inverse core/shell structure. In addition, the results show that, being encapsulated in a ~2 nm thick $CoFe_2O_4$ shell, the CoO core is successfully protected against oxidation which is crucial for the effectiveness of the magnetic coupling at the interface.

1. Introduction

Bimagnetic core/shell nanoparticles (NPs) have acquired increasing interest due to the possibility of combining different materials and fabricating nanostructures with improved properties [1,2]. The tuning of the magnetic properties through the interface coupling of distinct magnetic materials has been widely studied, mainly in thin films [3]. However, chemical advances in the fabrication of NPs that involve thermal decomposition methods of organometallic compounds [4,5] have allowed greater control of the synthesis and the possibility of designing new bimagnetic NPs suitable for the development of permanent magnets [6], data storage applications [7], spin-valve sensors [8] and biomedical uses [9–11]. Since nanostructured systems are very sensitive to surface and interface phenomena and the magnetic coupling mechanism at the interface is not fully understood [12,13], several experimental works have been focused on the relationship between the crystalline structure, the morphology and the physical properties [5,9,14,15]. In many cases, core/shell NPs have been fabricated by a controlled oxidation of single-phase NPs [16–18] but seed-mediated multi-steps methods have also been used [19,20] leading to greater versatility in the combination of different materials. Some experimental studies on materials involving magnetic phases with different crystalline structures and morphologies have been performed on core/shell [17,21], singly inverted core/shell [16], doubly inverted core/shell [22], cubic core/shell [15] or self-assembled [23] particles. The comprehension of the mechanisms that govern the magnetic behavior of these nanostructures is crucial for the development of engineered materials for innovative applications. Inverted core/shell bimagnetic systems are particularly interesting since they permit a greater control of the structural properties of its AFM core (and thus of the overall magnetic properties) that, in general, is not easily attained in conventional structures [24,25]. In particular, inverted core/shell $CoO/CoFe_2O_4$ particles formed by two highly anisotropic magnetic materials (antiferromagnetic – AFM – CoO and ferrimagnetic – FiM – $CoFe_2O_4$) have been reported as good candidates for increasing the magnetic hardness [19,26]. Since the origin of such coercivity increase is associated with the exchange interaction at the interface [26,27], the effectiveness of the magnetic coupling should be strongly related to the crystalline structure of the material and therefore to the synthesis process.

In this work we have fabricated bimagnetic $CoO/CoFe_2O_4$ nanoparticles by a seed-mediated synthesis method with the aim of investigating the influence of thermal annealing on the interface magnetic coupling that rules the magnetic properties of the system. We show how the magnetic behavior is strongly influenced by the chemical composition and crystalline structure of the system.

* Corresponding author. Tel.: +54 2944 445158.
E-mail address: lavorato@cab.cnea.gov.ar (G.C. Lavorato).

http://dx.doi.org/10.1016/j.jallcom.2015.02.050
0925-8388/

2. Experimental

$CoO/CoFe_2O_4$ core/shell nanoparticles were synthesized by means of the high-temperature decomposition of metal acetylacetonates assisted by oleic acid and oleylamine as surfactants. The procedure consists on the mixture of 4 mmol of $Co(acac)_2$, 8 mmol of oleic acid, 8 mmol of oleylamine, 0.02 mmol of 1–2 octanediol and 116 mmol of 1-octadecene. Subsequently, the mixture was magnetically stirred and heated up to 200 °C for 10 min, then, it was heated up again to the reflux temperature (315 °C) with a controlled heating rate of 30 °C min^{-1} and kept at that temperature for 120 min. Then, the mixture was cooled down to room temperature and a small portion of the obtained NPs was extracted for further analyses (sample *C*). In order to obtain core/shell NPs (sample *CF*), 0.8 mmol of $Co(acac)_2$ and 1.6 mmol of $Fe(acac)_3$ were added to the mixture according to the molar composition of the cobalt ferrite. In the same step, 0.02 mmol of 1–2 octanediol, 4 mmol of oleylamine, 4 mmol of oleic acid and 31 mmol of 1-octadecene were added and the preparation was heated up to 315 °C for another 120 min. In this second stage the heating rate was fixed at 30 °C min^{-1} to promote the heterogeneous nucleation of the spinel phase on the seeds.

Afterwards, the NPs were precipitated by centrifugation (14,000 rpm/30 min) and washed several times with a mixture of ethanol and toluene 8:1. With the objective of evaluating the effects of the thermal annealing on the magnetic properties of the core/shell NPs, both *C* and *CF* samples were heated up to 300 °C with a heating rate of 2.5 °C min^{-1} and kept at that temperature for 2 h in air atmosphere (samples *C–R* and *CF–R*, respectively). The obtained powder was then mixed with an epoxy resin to prevent the mechanical movement of the nanoparticles during the magnetic characterization.

The crystalline structure was characterized by X-ray powder diffraction (XRD), using a PANalytical Empyrean diffractometer (Cu Kα radiation). The core/shell morphology and particle size distribution were assessed by means of a Philips CM200 UT transmission electron microscope (TEM) operating at 200 kV. The crystallinity and morphology of the samples were evaluated by high-resolution and dark-field TEM images. The magnetic behavior was analyzed using a superconducting quantum interference device (SQUID, Quantum Design) magnetometer in the temperature range of 5–330 K and a LakeShore VSM with a ±10 kOe maximum applied field in the temperature range 250–320 K. Magnetization versus temperature experiments were performed following the ZFC (zero field cooling) and FC (field cooling) procedures for both as-produced and annealed samples at applied fields of 100 Oe and 5 kOe. TRM (thermoremanent magnetization) measurements were performed by cooling the sample from 330 to 5 K under 100 Oe applied field and subsequently measuring the magnetization during heating at zero applied field.

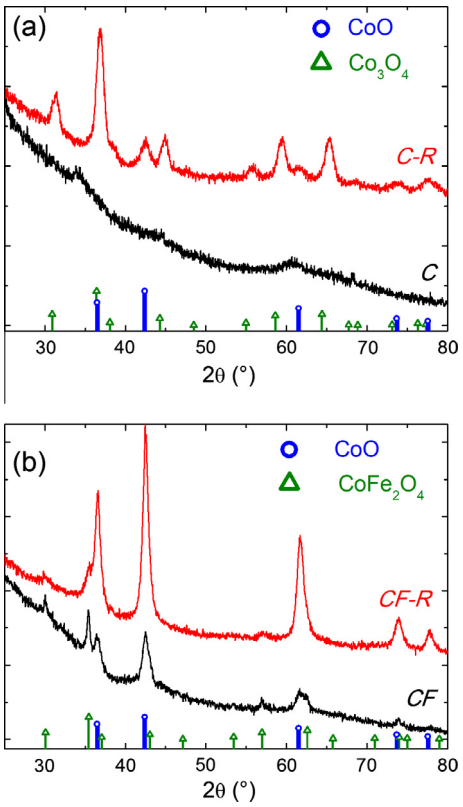

Fig. 1. X-ray diffraction patterns of (a) as-synthesized cores (C) and annealed cores (C–R) and (b) as-synthesized core/shell (*CF*) and annealed core/shell (*CF–R*) nanoparticles. Thick lines indicate the reflections for bulk CoO, $CoFe_2O_4$ and Co_3O_4.

3. Results

Fig. 1a shows the XRD patterns of the as-synthesized and thermal annealed CoO NPs, *C* and *C–R* samples respectively. For comparison, the diffraction peaks of bulk Fm-3m CoO and Fd-3m Co_3O_4 phases were included. In the as-synthesized sample only the diffraction peaks of the CoO phase could be identified which are broad and barely resolved. After the thermal treatment, although the CoO diffraction pattern is detected, the predominant phase is Co_3O_4 indicating that Co^{2+} was oxidized during the annealing. Fig. 1b shows the XRD patterns of the as-synthesized (*CF*) and annealed (*CF–R*) core/shell $CoO/CoFe_2O_4$ nanoparticles. The XRD peaks can be indexed by the bulk Fm-3m CoO and Fd-3m $CoFe_2O_4$ reflections. It is noteworthy from Fig. 1b that, after the annealing, the CoO diffraction peaks are notably better defined, narrower and their intensity grows relatively to the $CoFe_2O_4$ peaks, suggesting a higher degree of crystalline order for the CoO structure. Regarding the crystalline structure, it is observed that the diffraction peaks' positions of both phases for sample *CF* match well with the expected values of its bulk counterparts. However, after the thermal treatment, only CoO peaks reproduce the bulk positions, while $CoFe_2O_4$ peaks are broader and shifted approximately $\Delta(2\theta) \sim 0.2°$ from the expected bulk values. As a consequence, for example, the $CoFe_2O_4$ interplanar distance d_{311} calculated from the diffraction peak shift decreases from 2.534 Å to 2.524 Å after the annealing.

TEM micrographs corresponding to annealed core/shell NPs are shown in Fig. 2. The particle size dispersion was evaluated by measuring hundreds of particles and it is reported in Fig. 2a. The obtained histogram was fitted with a lognormal function and a mean size of 8.7 ± 1.9 nm was calculated. To analyze the core/shell structure, high resolution and dark field TEM images were measured and representative images are displayed in Fig. 2b–d. The $CoFe_2O_4$ shell morphology was confirmed by dark field images reconstructed by positioning a small objective aperture on the 111 $CoFe_2O_4$ diffraction ring. A shell thickness of ~2 nm was estimated from numerous dark field and HRTEM images. Moreover, the images reveal that the particles are separated by residual amorphous carbon from the synthesis that would prevent the coalescence of NPs. Finally, it should be noticed that the core/shell nanoparticle size is larger than ~7 nm NPs obtained by the same method but employing a different solvent with a lower reflux temperature [19].

Fig. 3 presents the magnetization measurements for *CF* and *CF–R* samples. The temperature dependence of the magnetization for the *CF* as-prepared sample, presented in Fig. 3a, shows the typical behavior of an assembly of weakly interacting magnetic nanoparticles, where the magnetic moments block progressively when the temperature diminishes according to their energy barrier distribution. The ZFC magnetization curve presents a maximum which is related to the mean blocking temperature, $\langle T_B \rangle$, and the FC magnetization increases when the temperature is decreased, as expected for non- or weakly-interacting particles. Moreover, a slight magnetization increase is observed at low temperature either for ZFC and FC curves; this feature is more evident when the measurement is performed with a higher applied field, as seen in Fig. 3c. The energy barrier distribution, showed in the inset of Fig. 3e, was obtained from the remanence curve according to: $f(T_B) \sim (1/T)[dM_{TRM}/dT]$, where $\langle T_B \rangle$ ~170 K was determined as the median value of the distribution [28] for the as-synthesized core/shell sample.

On the other hand, the magnetization of the annealed sample *CF–R*, presented in Fig. 3b, exhibits a different behavior. When